SHocks:
structure, AcceleRation, dissiPation

Work Package 4
Exploring acceleration in astrophysical shocks
through broadband emission

Deliverable D4.4
Technical report on the overall shock heating
properties of young SNRs as a function of Mach
number

Jacco Vink

Anton Pannekoek Institute & GRAPPA, University of Amsterdam, Science Park
904, 1098 XH Amsterdam, The Netherlands

21/12/2023

Document Change Record

Issue	Date	Author	Details
1	20/12/2023	J. Vink	

Table of Contents

Summary

We review here the shock heating properties of collisionless shocks in young SNRs, with a particular emphasis on the electron/ion temperature ratio. This being a measurable that can be reasonably well serve to compare SNR shock heating versus heliospheric shock heating. There are, however, some caveats since for SNR shocks we lack detail on the relevant length scales, and it is difficult to directly measure Mach numbers. Instead shock velocity are measured, which are then used to infer Mach numbers.

Apart from reviewing the observational situation and the physical process involved, we also show some recent SHARP results regarding both heliospheric and SNR electron/ion temperature ratio measurements.

1   Introduction

Heliospheric shocks and supernova remnant (SNR) shocks are collisionless, i.e. the transition in thermodynamic properties across the shock boundaries are not established by particle-particle collisions, mediated by Coulomb forces, but through collective electric and magnetic field fluctuations.

Both particle-in-cell simulations and in-situ observations of heliospheric show that the shock transition zone itself is of the order of the ion inertial length scale $l_{\mathrm{pi}} \sim c/\omega_{\mathrm{pi}} \approx 2.3 \times 10^2 n_{\mathrm{p}}\mathrm{km}$, or perhaps the ion gyroradius [Bale et al., 2003]. For comparison the ion-ion mean free path can be of the order of parsecs, i.e. even larger than the radii of young supernova remnants.

Thermodynamic equilibrium among plasma species, as governed by the Boltzmann equation, requires efficient particle-particle collisions. In the absence of these collisions it is not a priori clear whether all particle species can be described by one thermodynamic temperature, or even whether a Maxwellian distribution is an adequate distribution for the velocity distribution of all particles. From heliospheric data there is evidence that the kappa-distribution [Raymond et al., 2017] provides a better description. For SNRs the data quality is not good enough to establish non-Maxwellian distributions, but optical spectroscopy of SN1006 has provided some hints of non-Maxwellian proton distributions, and an hard X-ray tail to the spectrum of W49B also provides an hint of non-thermal tails to the electron distributions [Tanaka et al., 2018]. Moreover, it can be argued that the presence of cosmic rays accelerated by the shock itself also testifies of intrinsically non-Maxwellian features of the the particle energy distributions. However, we leave this issue alone for now, and for this technical report we assume that the bulk of the particles are reasonably well characterized by a temperature, but that this temperature depends on the particle species. We will discuss the influence that the cosmic-ray acceleration properties have on these temperatures.

In this report we will discuss the evidence for non-equilibrated electron-ion temperatures in SNRs and provide the link with heliospheric shocks. We also highlight some work on electron/ion heating done as part of the SHARP project. As we will see the determination of the shock heating processes in SNRs is difficult, but electron and temperatures as a function of shock properties still is one of the best measurables to compare heliospheric and SNR shocks.

2   General considerations regarding supernova remnant shock heating

Within the SHARP project most emphasize has been on the study of heliospheric shocks with in-situ data. Workpackage 4 is , concerned by exploring the differences or similarities with the collisionless shocks in young SNRs. It is good to establish first the similarities and differences between heliospheric and SNR shocks.

Both heliospheric and SNR shocks are collisionless shocks, and the shock transition zone length scale in both cases are probably similar, i.e. of the order of a few hundred kilometer. However, a big difference is that for heliospheric shocks the shock transition zone can be measured in considerable detail, as a spacecraft moves through the shock. Most of the relevant thermodynamic properties from upstream to downstream can be measured. For a given shock one usually has only one or perhaps multiply path through the shock.

2.1   Observational resolution

For SNR shocks one has to rely on multiwavelength data. For the shock properties the most important data come from optical and X-ray observations. The current best resolution is of the order of $0.5''$ with the Hubble Space Telescope or Chandra X-ray Observatory. For a young, relatively nearby SNR as SN1006, at 2 kpc, this resolution corresponds to a length scale of 1.5×10^{11} km, i.e. 1000 AU! Moreover, even a pencil beam of $0.5 \times 0.5''$ will cross plasma over a large scale. So at best we get plasma properties averaged over a long length scale. Apart from averaging over large volumes, on the $\gtrsim 1.5 \times 10^{11}$ km length scale some of the thermodynamic properties may also be affected due to fact that over these length scales there will be some electron-ion equilibration, which has a time scale of $\tau_{\mathrm{Coulomb,ep}} \approx \frac{T_i}{(dkT_i/dt)} \approx 3.15 \times 10^{11} n_{\mathrm{p}}^{-1} \left(\frac{k\overline{T}}{1\,\mathrm{keV}} \right)^{3/2}$. The typical young SNRs plasmas are characterized by an ionization age of $n_{\mathrm{e}}t \approx 10^{10}$–$10^{11}$ cm^{-3}s [Vink, 2020], which is comparable with $\tau_{\mathrm{Coulomb,ep}}$ for $n_{\mathrm{e}} \approx 1$–10 cm^{-3}.

To complicate the matter even further, X-ray spectroscopy provides the best means of measuring the plasma temperature. However, the temperature that is most easily measured is the electron temperature as this affects the line emission strength and line ratios, as well as the bremsstrahlung continuum shape. The ion temperature can be measured through Doppler broadening, but this requires high-resolution X-ray spectroscopy, and also requires to isolate regions of the SNR in which Doppler broadening due bulk motions along the line of sight is minimized.

2.2   Hydrogen excitation/ionization length scales for Balmer dominated shocks

Interestingly, spectroscopically one can zoom into SNR shocks more. This methods works for so-called Balmer-dominated shocks [see Heng, 2010, Vink, 2020, for reviews]. These are SNR shocks moving through a partial neutral medium. The neutral hydrogen atoms moving through the shock will eventually be ionized. However, a large fraction of the neutrals will first undergo an excitation by electron impact, or proton-hydrogen collisions may lead to charge-exchange reaction,
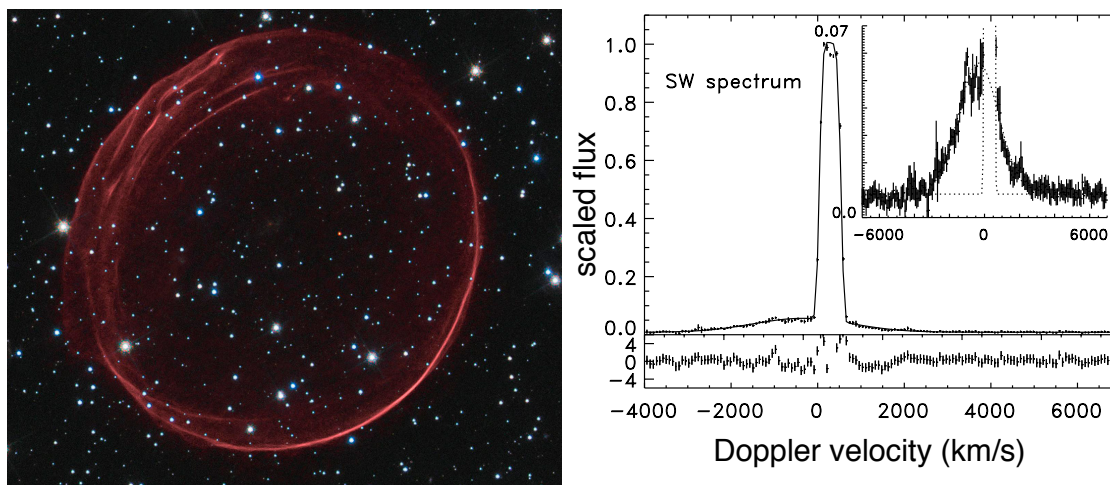
Figure 1: Left: In red, Hα emission from SNR 0509-67.5 [Hovey et al., 2015] , located in the Large Magellanic Cloud. The image is photomontaged on a broad band optical image, all taken with different instruments on board the *Hubble Space Telescope.* (Source: NASA, ESA, and the Hubble Heritage Team (STScI/AURA)/J.P. Hughes.) Right: Spectral line shape of Hα for the southwestern region of SNR 0509-67.5, taken with the ESO VLT/FORS2 instrument. The line shape consists of a narrow, plus a broad line (the latter shown in detail in the inset). The narrow line is not resolved, due to the wide spectral slit chosen, and the broad line is blueshifted with respect to the narrow line, as a result of a slight inclination of the post-shock flow toward us. (Reproduced from Helder et al. (2010) [Helder et al., 2010].)

leaving the newly formed atom usually in an excited state. The direct excitation happens to an atom that has not yet felt the presence of the shock, and as a result the Balmer lines caused by de-excitation will have a Doppler velocity and Doppler width indicative of the pre-shock gas velocity and temperature. This corresponds to a narrow emission line. On the other hand, the charge-exchange will result in an excited hydrogen atom that originate from a shock-affected proton. Hence, its Doppler properties are indicative of the post-shock temperature. And the charge-exchange will give rise to a broad line. An example of the superposition of a narrow and broad line is shown in Fig. 1, taken from [Vink, 2020].

So Balmer-dominated shocks allow for the measurements of the pre-shock temperature (from the narrow line), the post-shock proton temperature (broad line), whereas the ratio of the fluxes in the two lines can be used to measure the electron to ion temperature ratio [Heng, 2010, van Adelsberg et al., 2008].

The length scale over which these line excitation processes and final ionization occur is of the order of 10^{10} km, which is an order of magnitude better than the spatial resolution that can be obtained.

There is, however, a major drawback to using Balmer dominated shocks to study SNR shock thermodynamics: it requires the presence of an upstream gas that is (partially) neutral! The presence of neutrals has two effects: 1) it may dampend plasma fluctuations; 2) the shock transition layer extend now from the ion inertial length scale of hundreds of kilometers to a shock transition zone of the order of the ionization length scale, i.e. $\sim 10^{10}$ km. So a partial neutral shock

has an initial shock similar to an heliospheric shock, followed by a transition zone in which steadily more of the neutral kinetic energy is used to heat the initially neutral particles.

The charge-exchange reactions may also lead to another interesting phenomenon: as the post-shock protons likely have an isotropic distribution in the downstream shock frame, a charge exchange may lead to a neutral hydrogen atom that may move back toward the shock unhindered, and finally interact with the upstream gas [Raymond et al., 2011, Blasi et al., 2012]. There the neutrals may pre-heat the upstream plasma. This is yet another physical phenomenon that may result in difference in shock transition regions between Balmer-dominated shock and shocks moving completely in ionized plasma.

Interestingly, among the young SNRs only the Type Ia SNRs show Balmer dominated shocks, these include SN1006, SN1572 (Tycho's SNR) and SN1604 (Kepler's SNR). For several Balmer dominated shocks there is evidence that the upstream plasma temperature is higher than expected, suggesting some form of pre-heating [Sollerman et al., 2003].

2.3   The influence of cosmic-ray acceleration

SNRs are thought to be the dominant sources of Galactic cosmic rays. On average 5–10% of the available shock energy should be transferred to accelerated particles. During the acceleration cycle of particles, as a result of diffusive shock acceleration (DSA), an extensive shock precursor forms which will extend up to $l_{\mathrm{precursor}} \approx D_1/V_{\mathrm{s}}$, with D_1 the energy-dependent, upstream diffusion coefficient, and V_{s} the shock velocity. The length scales of these precursors can be up to 10% of the shock radius, so up to $\sim 10^{13}$ km. Also some heliospheric shocks are accompanied by accelerated particles, but the acceleration times are much shorter (hours to days rather than years), and hence the upstream length scales are shorter.

Depending on the energy available in cosmic rays, the upstream plasma may be pre-compressed and pre-heated, before the actual shock arrives. The question is whether to include this precursor into the shock transition region (like the foot region in heliospheric shocks), or only regard the actual shock (sometimes called subshock) as the relevant one. As indicated above, there is indeed evidence for pre-heating of the plasma in young SNRs. This may be caused by processes related to the cosmic-ray precursor.

The effect of efficient cosmic-ray acceleration will be that the postshock temperature will be lower than expected for a given shock velocity [e.g. Vink et al., 2010]:

$$kT_{\mathrm{downstream}} = (1-w)\frac{1}{\chi}\left[\frac{1}{\gamma M_{\mathrm{s}}^2} + \left(1 - \frac{1}{\chi}\right)\right]\mu m_{\mathrm{p}} V_{\mathrm{s}}^2, \tag{1}$$

with $w = P_{\mathrm{cr}}/P_{\mathrm{tot}}$ a measure of the cosmic-ray acceleration efficiency, M_{s} the sonic Mach number, and μm_{p} the mean particle mass. The temperature here is the mean temperature over all particle species. The number χ is the total compression ratio, which is $\chi \approx 4$ for strong shocks, but may in fact be higher if cosmic-ray acceleration is efficient. We see that for $M_{\mathrm{s}} \to \infty$, $\chi = 4$ and $w = 0$ this expression reduces to the well-known expresion

$$kT_{\mathrm{downstream}} = \frac{3}{16}\mu m_{\mathrm{p}} V_{\mathrm{s}}^2. \tag{2}$$

For efficient cosmic-ray acceleration we have $\chi > 4$ and $w > 0$, and the expression shows that the downstream temperature is reduced.

2.4 Mach numbers in heliospheric and supernova remnant shocks

From the thermodynamic point of view Mach numbers are one of the key ingredients for determining the post-shock plasma properties. In heliospheric shocks the most common Mach number used is the Alfvén Mach number, $M_{\mathrm{A}} = \sqrt{4\pi\rho V_s^2/B^2}$. M_{A} is more easily measured in heliospheric shocks than the sonic Mach number M_{s}. For young SNR shocks, however, neither M_{s} nor M_{A} can be directly measured. Young SNRs have strong shocks, implying that $\chi = 4$. At best we can measure downstream temperature and shock velocity through proper motion studies. As we see in Eq. 1 and 2, the temperature in the strong shock regime no longer depends on the Mach number.

Shock velocities have now been measured for most, if not all, young SNRs. As an example, during this SHARP project Vink carried out such a study all along the borders and interior of the Cas A SNR [Vink et al., 2022], where a mean forward shock velocity was found of ≈ 5800 km s^{-1}. Note that one needs an accurate distance measurement to convert proper motions into a shock velocity. For Cas A the distance is measured to be $d = 3.4 \pm 0.2$ kpc, but for example for Kepler's SNR there is some controversy regarding its distance [Vink, 2016].

When comparing the shock heating properties of heliospheric shocks to SNR shocks [e.g. Ghavamian et al., 2013, Vink et al., 2015] one used the measured shock velocity to infer a sonic Mach number, by assuming an upstream sound speed of 11 km s^{-1}. This is at best an educated guess. The reasoning is that the upstream medium is ionized by the SNR progenitor, or perhaps by the supernova event itself. It is well known that the cooling curve of cosmic plasma is such that a plasma cools rapidly from 100,000K to 10,000K, but that the cooling time is slow around 10,000K. So it is assumed that the upstream plasma has a temperature of 5000–10000K, corresponding to a sound speed of 10–15km s^{-1}. Young SNRs have shock velocities of $\gtrsim 2000$ km s^{-1}, so that the expected sonic Mach numbers are $M_{\mathrm{s}} \gtrsim 130$.

However, note that the measurements of narrow-line widths by Sollerman et al. [2003], cited already above, suggest that there may actually be quite some pre-shock heating in the precursor of up to 20,000-60,000 K, leading to an overestimate of M_{s} by a factor of 2, i.e. M_{s} could be typically around 50 for young SNRs. From an electron-ion equilibration point of view this is interesting as around $M_{\mathrm{s}} \approx 50$ there is a critical Mach number where the electron Mach number (i.e. electron thermal speed divided by shock speec) does exceed 1 [Vink et al., 2015].

Within the field of SNR studies little attempt has been made to infer Alfvén Mach numbers. We note here that the interstellar medium magnetic field is of the order of 5 μG, whereas for young SNRs the downstream magnetic-field measurements are of the order of 50–500 μG , with some evidence that the downstream magnetic field scales with the density as [Helder et al., 2012]

$$\frac{B^2}{8\pi} \approx K\sqrt{\rho_{\mathrm{upstream}}V_{\mathrm{s}}^2}. \tag{3}$$

However, a scaling with $B^2 \propto V_s^3$ is also consistent with the data [Helder et al., 2012]. It should be noted that the most likely cause of this scaling is the Bell instability induced by cosmic-ray streaming [Bell, 2004].

If we assume the scaling $B^2 \propto V_s^2$ and use Cas A as a bench mark ($\rho \approx 2m_p$ cm^{-3}, $B_{\text{upstream}} \approx 80$ μG, $V_s \approx 5800$ km s^{-1}), we find that $K \approx 2 \times 10^{-4}$. If now use Eq. 3 and insert it in the expression of the Alfvén Mach number we see that for young SNRs we expect a more or less constant Alfvén Mach number of $M_A \approx \sqrt{1/2K} \approx 70$. The number is benchmarked for Cas A, and shows that the Mach number is in the strong shock regime, despite the magnetic field amplification due to the Bell instability. This Mach number applies to the actual shock as compared to the plasma properties in the cosmic-ray precursor. If one considers the cosmic-ray precursor to be part of the shock transition zone than the Mach number is much larger.

3 Observations of shock heating in supernova remnants

As stated above the most common measurement of the postshock temperature concerns the *electron* temperature, based on thermal continuum shape and X-ray line ratios. The electron temperatures inferred from young SNRs are all $kT_e \lesssim 5$ keV [Vink, 2012], whereas for those young SNRs we typically have measured shock velocities $V_s \gtrsim 3000$ km s^{-1}, which according to Eq. 2 implies for electron-ion equilibration $kT_e \gtrsim 10$ keV.

A case in point is again Cas A, where the UvA group has recently investigate the circumstellar material shocked by the forward shock, and found that the electron temperatures are $0.7 \leq kT_e \leq 4.1$ keV (Vink et al in preparation, see also Mercuri A., MSc Thesis, 2023). For Cas A the relevant shock velocities are 4000–6000 km s^{-1}, corresponding to $kT_{\text{equilibrated}} \approx 18$–40 keV.

Another recent example, based on SHARP funded research is Tycho's SNR [Ellien et al., 2023], where for an X-ray synchrotron dominated shock region it was found that $kT_e = 0.96^{+1.33}_{-0.55}$ keV, whereas for the regions investigated temperatures of 10–15 keV are expected.

So clearly, the electron temperature is not in accordance with the expected postshock electron temperature for the case of full electron-ion temperature equilibration.

This leaves the explanation that electrons are much cooler than the ions, but an alternative explanation is that cosmic-ray acceleration leads to an overall low temperature, following Eq. 1. The latter seems unlikely as we need to have $w > 0.5$, which corresponds to a very high cosmic-ray acceleration efficiency.

However, to measure the actual electron over ion temperature ratio also the ion temperature needs to be measured. This can only be done by measuring the thermal Doppler broadening of lines. The most common measurements are for the Balmer lines in Balmer-dominated shocks using optical spectroscopy (Sect. 2.2). Overviews of the available measurements can be found in van Adelsberg et al. [2008], Ghavamian et al. [2013].

In addition one can measure the line broadening using UV data [e.g. Raymond et al., 1995] or in X-rays. In all cases the relation between ion temperature and

line broadening is

$$kT_\mathrm{i} = m_\mathrm{i}\sigma_\mathrm{v}. \tag{4}$$

Often the line broadening is given in full width at half maximum, related to σ_v as FWHM$=\sqrt{8\ln 2}\sigma_\mathrm{v}$).

The measurements in X-rays are difficult. One first needs to have a high resolution spectrometer. However, the grating spectrometers on board Chandra and XMM-Newton are slitless spectrometers, which are difficult to use for extended objects like SNRs. With the operations of XRISM [Tashiro et al., 2020] , which was launched in August 2023, a new type of high resolution spectrometers will be able to do better, but with the drawback that XRISM has a poor angular resolution of around $1'$. A problem with X-rays is also that care has to be taken to separate bulk velocity broadening from thermal Doppler broadening.

Despite the difficulties X-ray grating spectrometers have measured ion temperatures from a few young SNRs. For example, for a bright knot in SN1006 the oxygen temperature was found to be 200-500 keV [Vink et al., 2003, Broersen et al., 2013], whereas the electron temperature was much lower $kT_\mathrm{e} \approx 1.5$ keV. For SN1987A it was also inferred that the ion temperature was much higher than the electron temperature [Miceli et al., 2019]. However, in this case the bulk velocity broadening had to be corrected for using hydrodynamic simulations.

As part of the SHARP program the reflective grating spectrometer on board XMM-Newton was used to measure and model the line spectra of Kepler's SNR [Kasuga et al., 2021]. Here only slaps across the SNR could be analyzed and it was difficult to separate the bulk velocity line broadening from thermal Doppler broadening. However, the bulk velocities should be minimal in the outer regions. If the measured line broadening there is due to thermal Doppler broadening the implied oxygen temperature is $kT_\mathrm{O} \approx 900$ keV, consistent with no interspecies equilibration and a shock velocity of $V_\mathrm{s} \approx 2500\text{–}5000$ km s^{-1}, in agreement with proper motion measurements for that SNR [e.g. Vink, 2008].

The situation regarding the electron over ion temperature ratio has been subject to a recent review by Raymond et al. [2023], which lists many observations, mainly based on optical spectroscopy of Balmer dominated shocks. The overall trend noted in that paper, and in previous papers [Ghavamian et al., 2013, Vink et al., 2015] is that at low shock velocities the electron-ion temperature ratio is close to $T_\mathrm{e}/T_\mathrm{p} \approx 1$, whereas at very high shock velocities for SNRs the ratio drops to $T_\mathrm{e}/T_\mathrm{p} \approx 0.05$. Unlike for heliospheric shocks Raymond et al. [2023] note that for SNRs the $T_\mathrm{e}/T_\mathrm{p} \approx 1$ up to Mach numbers of 15–20. However, here we have to keep in mind that for SNRs it is possible to measure shock velocities, but for deriving Mach numbers several assumptions need to be made.

According to the model of Vink et al. [2015] the $T_\mathrm{e}/T_\mathrm{p} \approx 1$ for Mach numbers up to about 4 can be understood by electron heating due to adiabatic compression of the electrons. Above $M \gtrsim 4$ the shock compression has (nearly) reached its asymptotic value of 4, and adiabatic compression is maximimized. Only for $M \gtrsim \sqrt{m_\mathrm{p}/m_\mathrm{e}}$ does the bulk energy of the electrons alone contribute enough kinetic energy to heat up the electrons. All this is in the absence of additional electron heating due to energy exchange between electrons and ions, for example due to the electric cross shock potential.
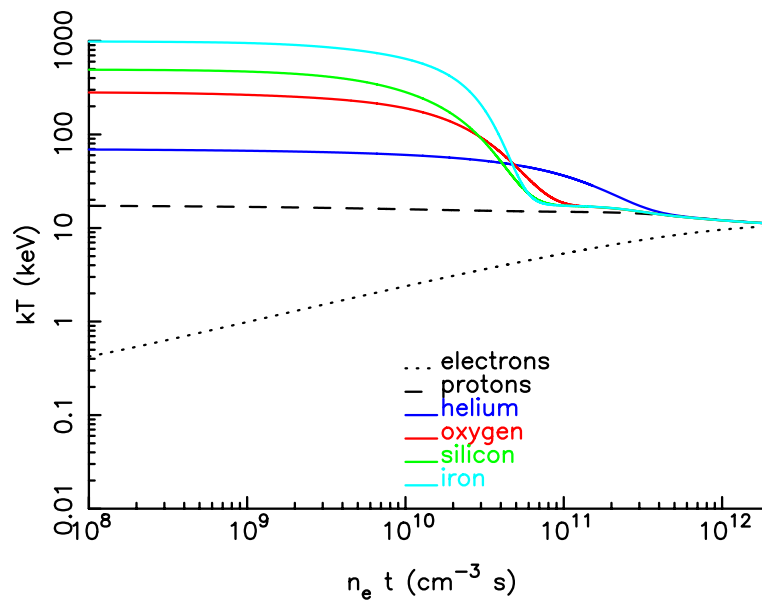
Figure 2: The temperature equilibration of different charged particles, as function of time: electrons (dotted line), protons (dashed) and various ions. The calculation assumes that each species i has an immediate post-shock temperature given by $kT_i = \frac{3}{16} m_i V_s^2$ with $V_s = 3000$ km s^{-1}. Subsequent equilibration occurs through Coulomb collisions on a time scale given by $n_e t \approx 10^{12}$ cm^{-3}s. It takes into account the time-dependent ionisation of the ions. Adiabatic or other losses are not taken into account.

3.1   Electron-ion temperature ratios at the reverse shock

The reverse shock is a shock that heats the gas coming from the supernova itself [McKee, 1974], and provides the inner boundary of the SNR shell. Initially the reverse shock moves outward in the frame of the observer, i.e. $dR_{rs}/dt > 0$, but after a few hundred to a few thousand years it moves inward [Truelove and McKee, 1999]. The thermodynamically important shock velocity is the relative speed with which the unshocked supernova ejecta enter the shock wave. This is given by the relative speed between the shock in the observer frame, and the velocity of the ejecta. The latter is simply the free expansion velocity, $v_{ejecta} = r/t = R_{rs}/t$, with t the age of the SNR. Hence, the thermodynamically important velocity is $V_s = R_{rs}/t - dR_{rs}/dt$.

The SHARP supported study of the shock velocities of Cas A [Vink et al., 2022] showed that in this young SNR the reverse shock moves outward in the eastern part of the SNR and inward in the western part. This is not expected for a wind density profile, and indicates some unusual wind evolution pattern for the progenitor of the supernova [Orlando et al., 2022]. Since the free expansion velocity of Cas A at the shock is quite high (~ 5000 km s^{-1}) and the western reverse shock is moving inward in the west the shock velocity is very high, up to $V_s \approx 8000$ km s^{-1}[Vink et al., 2022]. This is also the region in which the radio and X-ray synchrotron emission peaks, indicating very efficient particle acceleration.

From the point of shock heating the reverse shock is also interesting, as young SNRs like Tycho's SNR, Kepler's SNR and Cas A have reverse shocks that heat pure metal plasmas, i.e. consisting only of oxygen and or more massive elements. As a result the expected postshock temperature is much higher for a given shock velocity, as $\mu \gg 1$ in Eq. 2, compared to $\mu \approx 0.6$ for solar-composition plasmas.

Another reason why it is interesting for thermal Doppler broadening can be seen from the postshock equilibration evolution shown in Fig. 2. It shows that for a plane parallel shock with $V_s = 3000$ km s^{-1} the Coulomb equilibration time scale for full equilibration (including electrons) is about $\tau_{Coulomb,ei} \approx 32,000/n_e$ yr. But we also see that the ions among themselves equilibrate on a shorter time scale $\tau_{Coulomb,ii} \approx 3,200/n_e$ yr, due to larger charges Z involved and the smaller ratios of masses. So first the metal ions will equilibrate with the protons, and then all ions will equilibrate with the electrons. However, for the reverse shock there are no protons present, so the metals will remain considerably hotter for a longer time.

This could be of interest for Cas A, for which the plasma typically has $n_e t \approx 2 \times 10^{11}$ cm^{-3}s. For the forward shocked material we expect a much lower line broadening of the ions, as they will have equilibrated with the protons. However, for the reverse shock the ion line emission is expected to be significantly so ions should be equilibrated and electrons not for the forward shock.

This effect may already have been measured for Kepler's SNR in the aforementioned Kasuga et al. [2021], where it was found that the shocked ejecta component has a much larger line broadening than the shocked circumstellar medium. A drawback is that the reverse shock velocity is more difficult to measure through proper motion studies.

Note that with XRISM, and certainly in the more distant future with Athena, line broadening may be more routinely measured than is possible with the Chandra and XMM-Newton gratings.
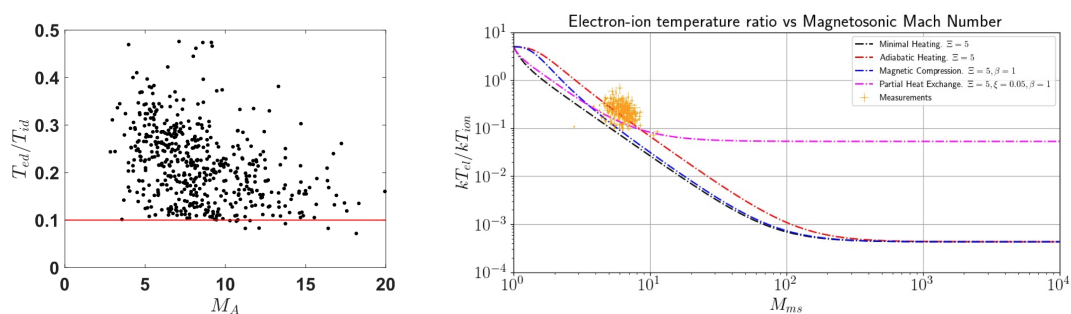
Figure 3: Left: The electron over ion temperature ratio for the Earth bowshock, based on MMS data. (Reproduced from Gedalin et al. [2023].) Right: Results obtained by Meuwissen et al., with comparison to modified model of Vink et al. [2015].

4 Comparing shock heating in heliospheric and supernova remnant shocks

The connection between heliospheric and young SNR shocks made within the SHARP is interesting as it potentially allows us to study collisionless shocks over a wide range of Mach numbers but with the caveat that for heliospheric shock Alfvén Mach numbers can be routinely measured, whereas for SNRs Mach numbers can only be crudely inferred.

Nevertheless the electron/ion temperature ratios is one of the best diagnostics to compare heating in heliospheric shocks with SNR shocks.

Since heliospheric shocks can be studied in detail, the heliospheric shocks can be used to disentangle the different contributions to electron heating, i.e. adiabatic heating, and heating due to cross shock potentials. These processes can even be followed along the shock transition trajectory [e.g. Johlander et al., 2023, another SHARP publication]. Within the SHARP project also MMS data of the Earth bowshock was used to investigate the electron versus ion heating [Gedalin et al., 2023]. Fig. 3 shows that there is quite some scatter in the electron-ion temperature ratio, but there is a trend that for higher Alfvén Mach number the ratio is decreasing, similarly to SNR measurements [Raymond et al., 2023], and theory [Vink et al., 2015]. However, there are still many complications. For example it is noted that the electron temperature first reaches a maximum after the overshoot and then seems to cool down. An important conclusions was that "electron heating does not follow the thermodynamic adiabatic law. The heating and cooling behavior implies that the energy is provided by the overall cross-shock potential while small-scale electric fields rapidly isotropize the electron distribution."

As part of the SHARP project there was also an exchange visit from the University of Amsterdam to Uppsala University by BSc student Daan Meuwissen. He investigated the electron/ion ratio using the SHARP data base, and results were published in his BSc thesis.[1] Also these results show there is quite a scatter in T_e/T_p ratios (Fig. 3, right), but with a trend to lower T_e/T_p for higher Mach numbers. An interesting finding by Meuwissen was that even upstream of the

---

[1] "The Electron-to-Ion Temperature Ratio in Collisionless Shocks, Measured by MMS" by Daan Meuwissen (2023). See `https://scripties.uba.uva.nl/search?id=record_53291`.

shock $T_e/T_p \neq 1$. This seems to commonly the case, but has not been taken into account in the shock heating theories like Vink et al. [2015].

Clearly what we lack currently is to cross the gap of Mach numbers of 10 to 100. Above $M = 100$ we have young SNRs, but the dynamic range with MMS is very limited. So other heliospheric shocks need to be investigated. On the SNR side one needs more observational data to correctly deduce Mach numbers from shock proper motions and upstream temperature diagnostics. With the new generation of X-ray spectrometers, such those of XRISM (recently launched) and Athena (to be launched beyond 2036) one can also X-ray data to measure ion temperatures. Currently most SNR measurements are confined to Balmer dominated shocks, which may have their own peculiarities, namely the presence of neutral atoms.

5   Conclusion

We have identified the electron/ion temperature ratio as a very interesting measurable quantity to compare heliospheric and SNR shocks, thereby encompassing a large range in Mach numbers. However, these comparison comes with some caveats, such as the lack of spatial details when it comes to studying SNR shocks, the over reliance on Balmer dominated shocks (which may behave differently due of the presence of neutrals), and the difficult in deducing Mach numbers from shock velocities, given the unknown upstream sound/Alfvén speeds.

As part of SHARP T_e/T_p measurements were made for the Earth bowshock. The overall the trend appears to be that T_e/T_p goes down with Mach number, but with considerable scatter. This is in agreement with SNR shocks, for reasonable choices of converting shock speeds to Mach number.

Clearly, the issue of T_e/T_p needs further attention, but SHARP shows that it is very fruitful to work on this area with a team consisting of physicists working on heliospheric and SNR shocks.

6   References

S. D. Bale, F. S. Mozer, and T. S. Horbury. Density-Transition Scale at Quasiperpendicular Collisionless Shocks. *Physical Review Letters*, 91(26):265004, December 2003. DOI:10.1103/PhysRevLett.91.265004.

A. R. Bell. Turbulent amplification of magnetic field and diffusive shock acceleration of cosmic rays. *MNRAS*, 353:550–558, September 2004.

P. Blasi, G. Morlino, R. Bandiera, E. Amato, and D. Caprioli. Collisionless Shocks in a Partially Ionized Medium. I. Neutral Return Flux and its Effects on Acceleration of Test Particles. *ApJ*, 755:121, August 2012. DOI:10.1088/0004-637X/755/2/121.

S. Broersen, J. Vink, M. Miceli, F. Bocchino, G. Maurin, and A. Decourchelle. The northwestern ejecta knot in SN 1006. *A&A*, 552:A9, April 2013. DOI:10.1051/0004-6361/201220526.

Amaël Ellien, Emanuele Greco, and Jacco Vink. Evidence for Thermal X-Ray Emission from the Synchrotron-dominated Shocks in Tycho's Supernova Remnant. *ApJ*, 951(2):103, July 2023. DOI:10.3847/1538-4357/accc85.

Michael Gedalin, Michal Golan, Jacco Vink, Natalia Ganushkina, and Michael Balikhin. Electron Heating in Shocks: Statistics and Comparison. *Journal of Geophysical Research (Space Physics)*, 128(9):e2023JA031627, September 2023. DOI:10.1029/2023JA031627.

Parviz Ghavamian, Steven J. Schwartz, Jeremy Mitchell, Adam Masters, and J. Martin Laming. Electron-Ion Temperature Equilibration in Collisionless Shocks: The Supernova Remnant-Solar Wind Connection. *SSRv*, 178(2-4):633–663, October 2013. DOI:10.1007/s11214-013-9999-0.

E. A. Helder, D. Kosenko, and J. Vink. Cosmic-ray Acceleration Efficiency versus Temperature Equilibration: The Case of SNR 0509-67.5. *ApJ*, 719:L140–L144, August 2010. DOI:10.1088/2041-8205/719/2/L140.

E. A. Helder, J. Vink, A. M. Bykov, Y. Ohira, J. C. Raymond, and R. Terrier. Observational Signatures of Particle Acceleration in Supernova Remnants. *SSRv*, 173:369–431, November 2012. DOI:10.1007/s11214-012-9919-8.

K. Heng. Balmer-Dominated Shocks: A Concise Review. *Publications of the Astronomical Society of Australia*, 27:23–44, March 2010. DOI:10.1071/AS09057.

L. Hovey, J. P. Hughes, and K. Eriksen. A Direct Measurement of the Forward Shock Speed in Supernova Remnant 0509-67.5: Constraints on the Age, Ambient Density, Shock Compression Factor, and Electron-ion Temperature Equilibration. *ApJ*, 809:119, August 2015. DOI:10.1088/0004-637X/809/2/119.

Andreas Johlander, Yuri V. Khotyaintsev, Andrew P. Dimmock, Daniel B. Graham, and Ahmad Lalti. Electron Heating Scales in Collisionless Shocks Measured by MMS. *GRL*, 50(5):e2022GL100400, March 2023. DOI:10.1029/2022GL100400.

Tomoaki Kasuga, Jacco Vink, Satoru Katsuda, Hiroyuki Uchida, Aya Bamba, Toshiki Sato, and John P. Hughes. Spatially Resolved RGS Analysis of Kepler's Supernova Remnant. *ApJ*, 915(1):42, July 2021. DOI:10.3847/1538-4357/abff4f.

C. F. McKee. X-Ray Emission from an Inward-Propagating Shock in Young Supernova Remnants. *ApJ*, 188:335–340, March 1974. DOI:10.1086/152721.

Marco Miceli, Salvatore Orlando, David N. Burrows, Kari A. Frank, Costanza Argiroffi, Fabio Reale, Giovanni Peres, Oleh Petruk, and Fabrizio Bocchino. Collisionless shock heating of heavy ions in SN 1987A. *Nature Astronomy*, 3:236–241, January 2019. DOI:10.1038/s41550-018-0677-8.

S. Orlando, A. Wongwathanarat, H. T. Janka, M. Miceli, S. Nagataki, M. Ono, F. Bocchino, J. Vink, D. Milisavljevic, D. J. Patnaude, and G. Peres. Evidence for past interaction with an asymmetric circumstellar shell in the young SNR Cassiopeia A. *A&A*, 666:A2, October 2022. DOI:10.1051/0004-6361/202243258.

J. C. Raymond, W. P. Blair, and K. S. Long. Detection of Ultraviolet Emission Lines in SN 1006 with the Hopkins Ultraviolet Telescope. *ApJ*, 454:L31–L37, November 1995. URL `http://adsabs.harvard.edu/cgi-bin/nph-bib_query?bibcode=1995ApJ...454L..31R&db_key=AST`.

J. C. Raymond, J. Vink, E. A. Helder, and A. de Laat. Effects of Neutral Hydrogen on Cosmic-ray Precursors in Supernova Remnant Shock Waves. *ApJ*, 731:L14+, April 2011. DOI:10.1088/2041-8205/731/1/L14.

J. C. Raymond, P. F. Winkler, W. P. Blair, and J. M. Laming. Ion-Ion Equilibration and Particle Distributions in a 3000 km s^{-1} Shock in SN 1006. *ApJ*, 851:12, December 2017. DOI:10.3847/1538-4357/aa998f.

John C. Raymond, Parviz Ghavamian, Artem Bohdan, Dongsu Ryu, Jacek Niemiec, Lorenzo Sironi, Aaron Tran, Elena Amato, Masahiro Hoshino, Martin Pohl, Takanobu Amano, and Frederico Fiuza. Electron-Ion Temperature Ratio in Astrophysical Shocks. *ApJ*, 949(2):50, June 2023. DOI:10.3847/1538-4357/acc528.

J. Sollerman, P. Ghavamian, P. Lundqvist, and R. C. Smith. High resolution spectroscopy of Balmer-dominated shocks in the RCW 86, Kepler and SN 1006 supernova remnants. *A&A*, 407:249–257, August 2003.

Takaaki Tanaka, Hiroya Yamaguchi, Daniel R. Wik, Felix A. Aharonian, Aya Bamba, Daniel Castro, Adam R. Foster, Robert Petre, Jeonghee Rho, Randall K. Smith, Hiroyuki Uchida, Yasunobu Uchiyama, and Brian J. Williams. NuSTAR Detection of Nonthermal Bremsstrahlung from the Supernova Remnant W49B. *The Astrophysical Journal*, 866(2):L26, Oct 2018. DOI:10.3847/2041-8213/aae709.

Makoto Tashiro, Hironori Maejima, Kenichi Toda, Richard Kelley, Lillian Reichenthal, et al. Status of x-ray imaging and spectroscopy mission (XRISM). In Jan-Willem A. den Herder, Shouleh Nikzad, and Kazuhiro Nakazawa, editors, *Space Telescopes and Instrumentation 2020: Ultraviolet to Gamma Ray*, volume 11444 of *Society of Photo-Optical Instrumentation Engineers (SPIE) Conference Series*, page 1144422, December 2020. DOI:10.1117/12.2565812.

J. K. Truelove and C. F. McKee. Evolution of Nonradiative Supernova Remnants. *ApJS*, 120:299–326, February 1999. URL `http://adsabs.harvard.edu/cgi-bin/nph-bib_query?bibcode=1999ApJS..120..299T&db_key=AST`.

M. van Adelsberg, K. Heng, R. McCray, and J. C. Raymond. Spatial Structure and Collisionless Electron Heating in Balmer-dominated Shocks. *ApJ*, 689:1089–1104, December 2008. DOI:10.1086/592680.

J. Vink. The Kinematics of Kepler's Supernova Remnant as Revealed by Chandra. *ApJ*, 689:231–241, December 2008. DOI:10.1086/592375.

J. Vink. Supernova remnants: the X-ray perspective. *A&A Rev.*, 20:49, January 2012. DOI:10.1007/s00159-011-0049-1.

J. Vink. Supernova 1604, Kepler's supernova, and its remnant. *Supernova 1604, Kepler's supernova, and its remnant (in Handbook of Supernovae, Springer (ArXiv:1612.06905))*, December 2016.

J. Vink. *Physics and Evolution of Supernova Remnants.* Astronomy and Astrophysics Library. Springer International Publishing, 2020. ISBN 9783030552299. URL https://books.google.nl/books?id=WgSYzQEACAAJ.

J. Vink, J. M. Laming, M. F. Gu, A. Rasmussen, and J.S. Kaastra. Slow temperature equilibration behind the shock front of SN 1006. *ApJ*, 587:31–34, April 2003. URL http://adsabs.harvard.edu/cgi-bin/nph-bib_query?bibcode=2003ApJ...584..758V&db_key=AST.

J. Vink, R. Yamazaki, E. A. Helder, and K. M. Schure. The Relation Between Post-shock Temperature, Cosmic-ray Pressure, and Cosmic-ray Escape for Non-relativistic Shocks. *ApJ*, 722:1727–1734, October 2010. DOI:10.1088/0004-637X/722/2/1727.

J. Vink, S. Broersen, A. Bykov, and S. Gabici. On the electron-ion temperature ratio established by collisionless shocks. *A&A*, 579:A13, July 2015. DOI:10.1051/0004-6361/201424612.

Jacco Vink, Daniel J. Patnaude, and Daniel Castro. The Forward and Reverse Shock Dynamics of Cassiopeia A. *ApJ*, 929(1):57, April 2022. DOI:10.3847/1538-4357/ac590f.